

Redox behavior of cerium in heteropolyoxotungstate complexes

Mark R. Antonio,^a L. Soderholm,^a Clayton W. Williams,^a Nushrat Ullah^b and Lynn C. Francesconi^b

^a Chemistry Division, Argonne National Laboratory, Argonne, IL 60439, USA.
 E-mail: mrantonio@anlchm.chm.anl.gov, soderholm@anlchm.chm.anl.gov,
 williams@anlchm.chm.anl.gov

^b Chemistry Department, Hunter College of the City University of New York, New York, NY 10021, USA. E-mail: lfrances@hejira.hunter.cuny.edu

Received 20th May 1999, Accepted 28th August 1999

In situ XAFS spectroelectrochemistry is used to characterize the oxidation state and coordination environment of cerium in two different heteropolytungstates, the Wells–Dawson [Ce(α -2-P₂W₁₇O₆₁)₂]¹⁷⁻ anion, and the Preyssler [CeP₅W₃₀O₁₁₀]¹²⁻ anion. Ce(III), coordinated to the Wells–Dawson framework, is oxidized at an applied potential of +0.37 V vs. Ag/AgCl. This is 1.15 V less than the Ce(IV)/Ce(III) standard reduction potential of +1.52 V vs. Ag/AgCl, demonstrating that Ce(IV) is stabilized in this heteropolyanion. In contrast, Ce(III) when encapsulated in the Preyssler anion is not oxidized at potentials higher than would be required for its oxidation in a non-complexing medium, indicating a stabilization of Ce(III). This is despite the 12- charge on the anion. The different redox behavior of Ce is understood in terms of the different coordination environments afforded by the two heteropolyanions. The relative importance of saturative coordination *versus* electrostatic stabilization in the redox behavior of these two complexes is discussed.

Introduction

Cerium has two accessible oxidation states, III and IV, in aqueous solution. Only strong oxidants like permanganate and peroxydisulfate can oxidize Ce(III). In mineral acids, the formal reduction potential of the Ce(IV)/Ce(III) couple can vary significantly from the standard reduction potential of +1.52 V vs. Ag/AgCl (+1.72 V vs. NHE).^{1,2} Couples ranging from -0.2 to +1.6 V vs. Ag/AgCl have been observed, and are dependent upon the details of complexation with the anions available in solution.^{3,4} Previous work has shown that selected heteropolyoxotungstates can significantly influence the redox behavior of complexed f ions.⁵⁻¹² Whereas there have been several hypotheses put forth to explain the shifts in reduction potential for different complexes,^{7,9,10} there is, as yet, no clear understanding of the mechanism(s) behind the stabilizing effects of selected heteropolyanions on f elements in different oxidation states.

Heteropolyoxotungstates are anionic molecular clusters composed of tungsten, oxygen, and, commonly, phosphorus. Typical sizes vary from 50–200 atoms and typical charges vary from -3 to -15.¹³⁻¹⁶ In 1971, Peacock and Weakley reported that heteropolyoxotungstates stabilize tetravalent cerium.⁵ This stabilization was evident by the ease of oxidation of Ce(III) in [Ce(W₅O₁₈)₂]⁹⁻, [Ce(SiW₁₁O₃₉)₂]¹³⁻, [Ce(PW₁₁O₃₉)₂]¹¹⁻, and [Ce(P₂W₁₇O₆₁)₂]¹⁷⁻. In aqueous solutions, these oxidations were found to occur at +0.6 to +0.9 V vs. Ag/AgCl,⁵ which is less than the standard reduction potential of Ce(IV). More recently, Haraguchi *et al.*⁹ have confirmed the shifts of the Ce(IV)/Ce(III) redox potentials in these heteropolytungstates. The implication of their work is that the oxidation of Ce(III) is possible with the use of only mild oxidants. In contrast to this behavior, Eu(III) complexed in [EuP₅W₃₀O₁₁₀]¹²⁻ is more easily reduced to Eu(II) than is Eu(III) in a non-complexing electrolyte,^{11,17} and Eu(III) in [Eu(As₂W₁₇O₆₁)₂]¹⁷⁻ is not reducible.¹⁸ In order to obtain insights about the different redox chemistry of f-element heteropolytungstates, we compare herein the bulk solution response and coordination of cerium in [Ce(α -2-P₂W₁₇O₆₁)₂]¹⁷⁻ and [CeP₅W₃₀O₁₁₀]¹²⁻ at controlled-electrochemical potentials.

Heteropolyanion complexes with cerium are numerous.^{5-7,9,19-28} The two chosen for this study are the cerium analogs of the lanthanide series of monovacant, lacunary Wells–Dawson anions [Ln(α -2-P₂W₁₇O₆₁)₂]¹⁷⁻ and Preyssler anions [LnP₅W₃₀O₁₁₀]¹²⁻.^{8,25,29,30} These form heteropoly blues,³¹ as manifested by the blue color of their solutions upon reduction, which means that their P–W–O frameworks are electroactive. Although the details are different for the voltammetry exhibited by the Wells–Dawson and Preyssler anion clusters, the cyclic voltammograms from isostructural compounds appear similar irrespective of the identity of Ln.^{8,12,32-34} The exceptions to this behavior are the Ln = Ce member of the Wells–Dawson series^{9,10} and Ln = Eu member of the Preyssler series.^{8,11,17,35} CV data have been used to determine that Ce(III) in the complex [Ce(P₂W₁₇O₆₁)₂]¹⁷⁻ is oxidized at a potential (*E*_{1/2}) of +0.365 V vs. Ag/AgCl in an aqueous electrolyte at pH 4.5.⁹ The stability of Ce(IV) in [Ce(P₂W₁₇O₆₁)₂]¹⁶⁻ is attributed to the large negative charge on the Wells–Dawson anion.

The redox behavior of Ce associated with the Preyssler anion stands in contrast to that reported for the Wells–Dawson complex. Creaser *et al.*⁸ reported that tetravalent cerium in [CeP₅W₃₀O₁₁₀]¹¹⁻ could not be reduced to Ce(III) at any potential between -1.4 and +1.8 V vs. Ag/AgCl. An unprecedented stabilization of Ce(IV) was inferred from this work. Our studies²⁵ have shown that it is trivalent cerium, and not tetravalent cerium, that is incorporated into the Preyssler anion under the conditions reported in ref. 8. The presence of Ce(III) in the Preyssler anion explains why attempts to reduce cerium were ultimately unsuccessful.^{8,25} Nevertheless, the fact that there are no Ce(IV)/Ce(III) redox waves in the cyclic voltammetry data for [CeP₅W₃₀O₁₁₀]¹²⁻ suggests that Ce(III) cannot be oxidized, despite the large negative charge on the cluster.

Inorganic syntheses with Ce(III) and Ce(IV) oftentimes lead to new materials with unanticipated valences, such as Ce(III) in substituted cerocene complexes,³⁶ and in which the valence of Ce is not evident.³⁷ Examples in polyoxoanion chemistry include the Ce(III) complexes [CeP₅W₃₀O₁₁₀]¹²⁻ and

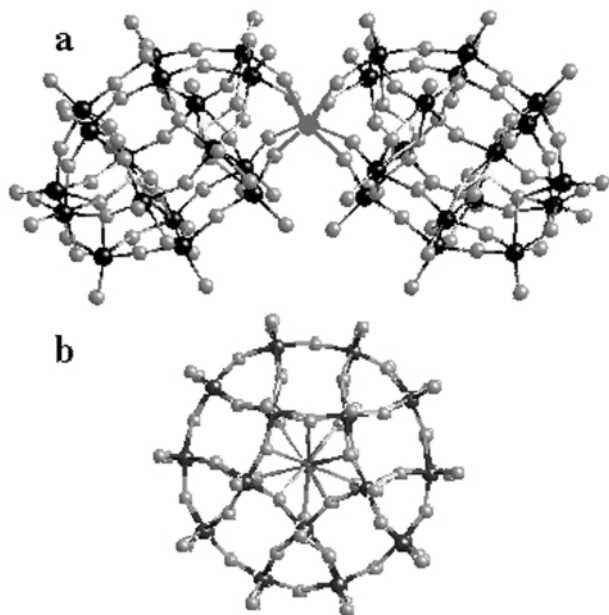


Fig. 1 (a) Structure of $[\text{Ce}(\alpha\text{-}2\text{-P}_2\text{W}_{17}\text{O}_{61})_2]^{16-}$ showing 8-fold O coordination of Ce(IV), center sphere, by two tetradentate polyoxoanions $[\alpha\text{-}2\text{-P}_2\text{W}_{17}\text{O}_{61}]^{10-}$,²² which are known as monovacant, lacunary Wells–Dawson anions. (b) Structure of $[\text{CeP}_5\text{W}_{30}\text{O}_{110}]^{12-}$ showing 10-fold O coordination of Ce(III), center sphere, inside the central tunnel-like cavity of the P–W–O framework of the Preyssler polyoxoanion.^{8,54}

$[\text{Ce}\{\text{Mo}_5\text{O}_{13}(\text{OME})_4(\text{NO})\}_2]^{3-}$, which were incorrectly cited as Ce(IV) complexes in the first reports.^{8,38} Valence ambiguities can also arise from the combination of Ce(IV)/Ce(III) redox activity with the multivalent 4d and 5d transition elements Mo and W in discrete polyoxoanion clusters and in extended, condensed solids. In early accounts, the behavior of Ce(IV) in $[\text{CeMo}_{12}\text{O}_{42}]^{8-}$ upon reduction of the anion and the valence of Ce in Ce_2MoO_6 were matters of some speculation. Now, it is known that both systems contain Ce(III).^{6,39} In general, the determination of the oxidation state of cerium in matter is frequently a difficult problem. Except through use of Ce XANES, which is a direct spectroscopic probe of cerium valence, the application of ESR, electronic and infrared spectroscopies as well as magnetic measurements, cyclic voltammetry and controlled potential electrolysis, *etc.*, can be troublesome. Both K- and L-edge Ce XANES have proven their strengths in resolving questions about the valence of Ce in studies of importance to inorganic chemistry,^{25,36,40–43} material sciences,^{39,44–48} catalysis,^{49–51} and corrosion^{52,53} research.

Here, using *in situ* XAFS spectroelectrochemistry, we contrast the redox properties and coordination environments of Ce in $[\text{Ce}(\alpha\text{-}2\text{-P}_2\text{W}_{17}\text{O}_{61})_2]^{17-}$ and $[\text{CeP}_5\text{W}_{30}\text{O}_{110}]^{12-}$. Through Ce L-edge XANES, we confirm that Ce(III) in the Wells–Dawson anion complex is reversibly oxidized and reduced at +0.37 V *vs.* Ag/AgCl in a supporting electrolyte of 0.1 M sodium sulfate at pH 5.7. Under these conditions, the non-complexed Ce(III) aqua ion is not oxidized. Conversely, Ce(III) in the cerium-exchanged Preyssler anion is not electroactive. It is not oxidized to Ce(IV) even under rigorous conditions of potential (+1.7 V *vs.* Ag/AgCl) and electrolyte (1 M HClO₄ sparged with O₂). These conditions are sufficient to oxidize the non-complexed Ce(III) aqua ion. Through use of Ce L-edge EXAFS, we found that the framework O coordination of Ce(III) and Ce(IV) in $[\text{Ce}(\alpha\text{-}2\text{-P}_2\text{W}_{17}\text{O}_{61})_2]^{17-16-}$ adjusts to accommodate the different radii of the Ce cations. In these two complexes, Ce is 8-coordinate. As shown in Fig. 1a, Ce is bound between two tetradentate $[\alpha\text{-}2\text{-P}_2\text{W}_{17}\text{O}_{61}]^{10-}$ polyoxoanions.²² In the Preyssler anion, the framework oxygen coordination of Ce(III) involves long interactions with 10 O atoms inside the tunnel-like cavity of the polyoxoanion.^{8,54} This Ce coordination is illustrated in Fig. 1b. The results of the work reported here provide insights

that may ultimately lead to a predictive understanding of the mechanisms by which a heteropolyanion affects the redox response of a complexed f ion.⁵⁵

Experimental

The cerium(III)-containing heteropolyoxotungstates were prepared according to literature methods.^{25,29} Phosphorus-31 NMR revealed the preparation of isomerically pure $[\text{Ce}(\alpha\text{-}2\text{-P}_2\text{W}_{17}\text{O}_{61})_2]^{17-}$ and single phase $[\text{CeP}_5\text{W}_{30}\text{O}_{110}]^{12-}$. Dilute aqueous solutions of 4 mM $[\text{Ce}(\alpha\text{-}2\text{-P}_2\text{W}_{17}\text{O}_{61})_2]^{17-}$ in 0.1 M Na₂SO₄ (anhydrous, Mallinckrodt) at pH 5.7 and 5 mM $[\text{CeP}_5\text{W}_{30}\text{O}_{110}]^{12-}$ in 1 M HClO₄ (Optima) were contained in a purpose-built spectroelectrochemical cell for *in situ* XAFS.⁵⁶ The XAFS experiments were performed at X-10C/NSLS and 4-3/SSRL with Si(220) monochromators. Ce L-edge fluorescence XAFS was collected using an ion chamber fluorescent detector without slits and filter.⁵⁷ The 8 keV mirror cut-off used at X-10C effectively eliminated harmonic leakage, and Ce L₃ XAFS was obtained without interference from the W L₂-edge response. Even with monochromator detuning of ≥80%, the W L₂-edge was evident in the Ce L₃ XAFS obtained at 4-3. In order to avoid this interference, we obtained Ce L₂ XAFS. The EXAFS was analyzed in the usual manner⁵⁸ with EXAFSPAK⁵⁹ using single-scattering phase and amplitude functions calculated with FEFF6.01a^{60,61} and a scale factor of 0.9.

Attempts to reproduce the cyclic voltammograms for $[\text{Ce}(\alpha\text{-}2\text{-P}_2\text{W}_{17}\text{O}_{61})_2]^{17-}$ using a glassy carbon working electrode (3.0 mm diameter, BAS MF-2012) following the procedures outlined by Haraguchi *et al.*⁹ were unsuccessful. By substituting a carbon rod working electrode (6.15 mm diameter, Alfa 14739) for the glassy carbon one, we were able to reproduce the CV data of Haraguchi *et al.*⁹ All bulk electrolysis and CV measurements were performed using these carbon rods for the working and auxiliary electrodes and a Ag/AgCl reference electrode (3 M NaCl, BAS RE-5B) with a BAS 100B/W electrochemical workstation. All subsequent potentials are given with respect to this reference electrode, which has a redox potential of +0.196 V *vs.* NHE at 25 °C.⁶² The cyclic voltammograms were obtained in static electrolytes, whereas the *in situ* bulk electrolysis was performed with vigorous sparging with He (for $[\text{Ce}(\alpha\text{-}2\text{-P}_2\text{W}_{17}\text{O}_{61})_2]^{17-}$) and O₂ (for $[\text{CeP}_5\text{W}_{30}\text{O}_{110}]^{12-}$). Exhaustive, reversible electrolysis of $[\text{Ce}(\alpha\text{-}2\text{-P}_2\text{W}_{17}\text{O}_{61})_2]^{17-}$ was achieved in less than 3 h as determined from the coulometry and amperometry. The shapes of the charge *vs.* time and current *vs.* time plots indicate no chemical reactivity for the electrolyzed species.

Results

$[\text{Ce}(\alpha\text{-}2\text{-P}_2\text{W}_{17}\text{O}_{61})_2]^{n-}$

The cyclic voltammogram for $[\text{Ce}(\alpha\text{-}2\text{-P}_2\text{W}_{17}\text{O}_{61})_2]^{17-}$ is shown in Fig. 2a. It reveals a redox wave at $E_{1/2} = +0.37$ V and three waves at potentials less than −0.2 V. The former is attributable to the Ce(IV)/Ce(III) redox couple and the latter are due to the redox activity of the P–W–O framework.⁹ The Ce L₃ XANES for the 4 mM solution of $[\text{Ce}(\alpha\text{-}2\text{-P}_2\text{W}_{17}\text{O}_{61})_2]^{17-}$ in 0.1 M Na₂SO₄ at pH 5.7 is shown in Fig. 2b. At the rest potential of +0.08 V (as indicated on Fig. 2a with arrow 1), the XANES for the pink solution of $[\text{Ce}(\alpha\text{-}2\text{-P}_2\text{W}_{17}\text{O}_{61})_2]^{17-}$ reveals a single sharp resonance at ≈5729 eV. This is typical of the XANES response for trivalent cerium.^{11,39} After exhaustive electrolysis at +0.6 V (indicated on Fig. 2a with arrow 2), the XANES for the yellow solution reveals two resonances at ≈5733 and 5740 eV. This response is typical for the XANES of tetravalent Ce, and indicates that the redox couple at +0.37 V in the CV data of Fig. 2a is due to the oxidation of Ce(III) in $[\text{Ce}(\alpha\text{-}2\text{-P}_2\text{W}_{17}\text{O}_{61})_2]^{17-}$ to Ce(IV) $[\text{Ce}(\alpha\text{-}2\text{-P}_2\text{W}_{17}\text{O}_{61})_2]^{16-}$. The

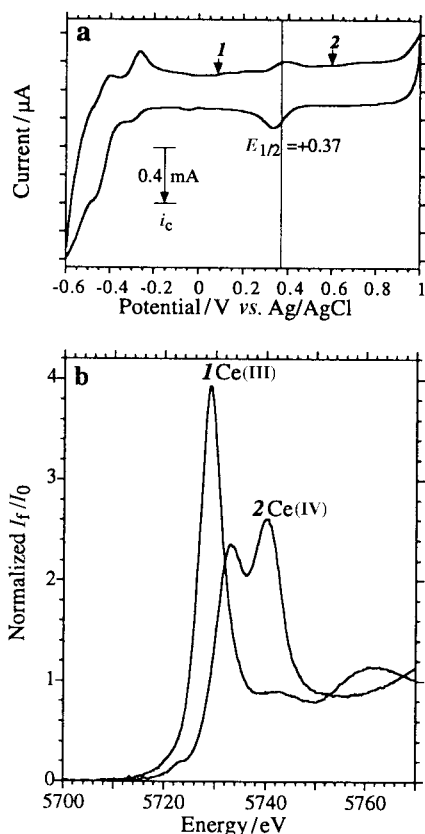


Fig. 2 (a) Cyclic voltammogram of $[\text{Ce}(\alpha\text{-}2\text{-P}_2\text{W}_{17}\text{O}_{61})_2]^{17-}$ obtained in an aqueous supporting electrolyte of 0.1 M Na_2SO_4 at pH 5.7, $\nu = 0.1 \text{ V s}^{-1}$. Arrows 1 and 2 indicate the rest potential (+0.08 V) and the potential (+0.6 V) applied for bulk electrolysis, respectively. (b) *In situ* Ce L_3 -edge fluorescence XANES obtained at ambient temperature for a 4 mM solution of $[\text{Ce}(\alpha\text{-}2\text{-P}_2\text{W}_{17}\text{O}_{61})_2]^{17-}$ in 0.1 M Na_2SO_4 at pH 5.7 at the rest potential (curve 1) showing trivalent cerium and after bulk electrolysis with the electrode polarized at +0.6 V (curve 2) showing tetravalent cerium.

oxidation was found to be reversible. Upon reduction of $[\text{Ce}(\alpha\text{-}2\text{-P}_2\text{W}_{17}\text{O}_{61})_2]^{16-}$ at +0.1 V, the resulting cerium XANES for the pink solution is indistinguishable from that initially obtained at rest potential. This reversibility is consistent with the observed reproducibility of the voltammetric behavior of $[\text{Ce}(\text{P}_2\text{W}_{17}\text{O}_{61})_2]^{17-}$.

The $k^3\chi(k)$ EXAFS and the corresponding Fourier transform data for $[\text{Ce}(\alpha\text{-}2\text{-P}_2\text{W}_{17}\text{O}_{61})_2]^{17-}$ with Ce(IV) ($n = 16$) and Ce(III) ($n = 17$) are shown in Fig. 3. The primary data of Fig. 3a (solid lines) are limited to a maximum of $\approx 8 \text{ \AA}^{-1}$ in k -space due to the onset of the Ce L_2 -edge. Nevertheless, differences between the Ce(IV) and Ce(III) coordination in the heteropolytungstate complex are evident in the Fourier transform (FTs) of Fig. 3b (solid lines). The peak due to the nearest O atoms about Ce(IV), upper curve, is more intense and at a shorter distance than the Ce(III)-O peak, bottom curve. Fitting the $k^3\chi(k)$ EXAFS provides the metrical information shown in Table 1. To obtain these results, we performed conservative 3-parameter, single-shell (Ce-O) fits. The limited data range available for analysis necessitated this conservative approach. The oxygen coordination numbers were fixed at 8 based upon evidence from a partial single-crystal X-ray diffraction measurement of $\text{K}_{16}[\text{Ce}(\text{P}_2\text{W}_{17}\text{O}_{61})_2] \cdot 50\text{H}_2\text{O}$, which reveals that Ce(IV) is bound to 4 O atoms from each of two $[\text{P}_2\text{W}_{17}\text{O}_{61}]^{10-}$ anions in a square antiprism geometry.²² The resolution of our data is estimated to be $\approx 0.3 \text{ \AA}$, so that Ce-O distances separated by less than this amount will produce a single peak in the FT that reflects the mean distance of the Ce-O interactions.

The best fits to the EXAFS data are shown as dashed lines in Fig. 3. It is clear from Fig. 3b that the conservative model we have used to fit the experimental Ce-O interactions is a good

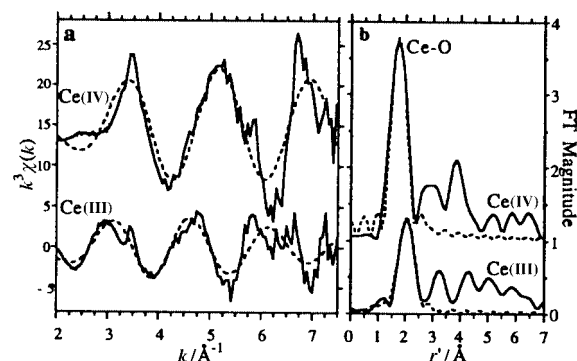


Fig. 3 *In situ* Ce L_3 -edge (a) $k^3\chi(k)$ EXAFS and (b) FT data for 4 mM aqueous solutions of $[\text{Ce}^{\text{III}}(\alpha\text{-}2\text{-P}_2\text{W}_{17}\text{O}_{61})_2]^{17-}$ (bottom curves) and $[\text{Ce}^{\text{IV}}(\alpha\text{-}2\text{-P}_2\text{W}_{17}\text{O}_{61})_2]^{16-}$ (top curves—offset for clarity), which were obtained at the rest potential of +0.08 V and after bulk electrolysis with the electrode polarized at +0.6 V, respectively. The solid lines are the primary experimental data and the dashed lines illustrate the fit.

representation of the data. Although we believe that the first two or three peaks beyond the strong O peak in the FT data of Fig. 3b have structural significance, the limited data range preclude a quantitative curve fitting analysis of these distant interactions. The data of Table 1 show that the average Ce(III)-O bond length of $2.52 \pm 0.04 \text{ \AA}$ is significantly longer than the average Ce(IV)-O distance of $2.27 \pm 0.02 \text{ \AA}$. Consistent with this, the Ce(III)-O bond has a larger mean-square deviation, as evidenced by its Debye-Waller factor, $0.014 \pm 0.004 \text{ \AA}^2$, which is about 3 times that for the Ce(IV)-O bond, $0.004 \pm 0.002 \text{ \AA}^2$.

$[\text{CeP}_5\text{W}_{30}\text{O}_{110}]^{12-}$

The cyclic voltammogram for $[\text{CeP}_5\text{W}_{30}\text{O}_{110}]^{12-}$ is shown in Fig. 4a. It reveals five closely spaced redox waves at potentials below 0 V, which are attributable to the redox activity of the P-W-O framework.^{8,25} From 0 to +1.9 V there are no other waves evident in the CV data of Fig. 4a. The rising slope at the most positive potentials is due to the onset of O_2 evolution. The Ce L_2 XANES for the 5 mM solution of $[\text{CeP}_5\text{W}_{30}\text{O}_{110}]^{12-}$ in 1 M HClO_4 is shown in Fig. 4b. At the rest potential of +0.53 V (as indicated on Fig. 4a with arrow 1), the XANES for the light-yellow solution (solid line) reveals a single sharp resonance at $\approx 6166 \text{ eV}$. Identical responses were observed throughout the bulk electrolysis experiments at potentials of +1.7 and -0.55 V, which are indicated on Fig. 4a with arrows 2 and 3, respectively. The Ce XANES obtained at rest potential (solid line, Fig. 4b) and with the electrode polarized at +1.7 V (dashed line, Fig. 4b) and -0.55 V (not shown) all reveal the presence of trivalent cerium. Under the electrochemical conditions employed herein, Ce(III) is not oxidized when contained within the Preyssler heteropolyoxotungstate anion. The XANES results confirm the interpretation based on the CV data that Ce is not redox active between -0.6 and +1.9 V.

The $k^3\chi(k)$ EXAFS and the corresponding FT data for $[\text{CeP}_5\text{W}_{30}\text{O}_{110}]^{12-}$ at rest potential are shown in Fig. 5a and b, respectively, as solid lines. After constant potential electrolysis at +1.7 V, the $k^3\chi(k)$ EXAFS and FT data (not shown) are indistinguishable from the data obtained at rest potential. The FT of Fig. 5b reveals one strong peak that is due to the O atoms about Ce(III). Metrical parameters were obtained using the simple, conservative approach that was used to fit the Wells-Dawson EXAFS. The best fits to the EXAFS data are shown as dashed lines in Fig. 5, and the results are listed in Table 1. In this complex, the oxygen coordination number was fixed at 10; chosen based upon evidence from single-crystal X-ray diffraction measurements of $[\text{EuP}_5\text{W}_{30}\text{O}_{110}]^{12-}$, which reveal that Eu(III) is bound to 10 O atoms inside the tunnel surface of the donut-shaped P-W-O framework.⁵⁴ By analogy with the Eu analog,⁵⁵ there may be water molecules within the tunnel,

Table 1 Curve fitting results for the *in situ* Ce L_{2,3}-edge solution EXAFS, $k^3\chi(k)$, of $[\text{Ce}(\alpha\text{-}2\text{-P}_2\text{W}_{17}\text{O}_{61})_2]^{n-}$ with Ce(III) ($n = 17$) and Ce(IV) ($n = 16$), and $[\text{CeP}_5\text{W}_{30}\text{O}_{110}]^{12-}$ ^a

Anion	E^b/V	N_{O}^c	$r^d/\text{\AA}$	$\sigma^2^e/\text{\AA}^2$	$\Delta E_0^f/\text{eV}$
$[\text{Ce}^{\text{III}}(\alpha\text{-}2\text{-P}_2\text{W}_{17}\text{O}_{61})_2]^{17-}$	+0.08	8	2.52(4)	0.014(4)	1.4
$[\text{Ce}^{\text{IV}}(\alpha\text{-}2\text{-P}_2\text{W}_{17}\text{O}_{61})_2]^{16-}$	+0.6	8	2.27(2)	0.004(2)	-2.9
$[\text{CeP}_5\text{W}_{30}\text{O}_{110}]^{12-}$	+0.53	10	2.70(3)	0.005(3)	3.7

^a The numbers in parentheses represent the estimated 95% confidence limits (3σ) obtained from the least-squares fit.⁵⁹ The number of curve fitting parameters ($3; r, \sigma^2, \Delta E_0$) was less than the number of independent data points, $N_{\text{dep}} = 2\Delta k\Delta r/\pi = 7$, where $\Delta k = 5.5 \text{ \AA}^{-1}$ and $\Delta r \approx 2 \text{ \AA}$. ^b The potential in V vs. Ag/AgCl. ^c The average number of oxygen atoms coordinated to Ce. These values were fixed for the curve fitting. ^d The average Ce–O bond length. ^e The Debye–Waller factor, which is the mean square deviation in the average Ce–O bond length. ^f The energy difference between the EXAFS experiment and FEFF theory.^{60,61}

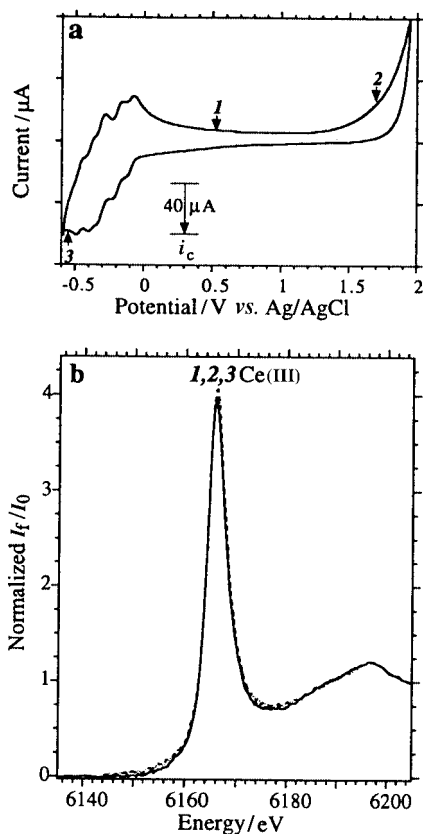


Fig. 4 (a) Cyclic voltammogram of $[\text{CeP}_5\text{W}_{30}\text{O}_{110}]^{12-}$ obtained in an aqueous supporting electrolyte of 1 M HClO_4 , $v = 0.1 \text{ V s}^{-1}$. Arrows 1 and 2, 3 indicate the rest potential (+0.53 V) and the potentials (+1.7 and -0.55 V) applied for bulk electrolysis, respectively. (b) *In situ* Ce L₂-edge fluorescence XANES obtained at ambient temperature for a 5 mM solution of $[\text{CeP}_5\text{W}_{30}\text{O}_{110}]^{12-}$ in 1 M HClO_4 at the rest potential (solid line) and after bulk electrolysis with the electrode polarized at +1.7 V (dashed line). The XANES data at all three potentials (arrows 1, 2, 3 in (a)) reveal trivalent cerium.

one or more of which may be bound to Ce. We are not able to determine the coordination number with enough accuracy to resolve this issue. Judging from previous studies,⁴⁶ it may be possible to further investigate the hydration of encrypted Ce using cerium K-edge EXAFS. Nevertheless, it is evident from the match between the experimental and fitted data of Fig. 5b that the modeling of the Ce–O interactions with 10 O neighbors is satisfactory. The average Ce(III)–O bond length is rather long, $2.70 \pm 0.03 \text{ \AA}$, yet the Debye–Waller factor, $0.005 \pm 0.003 \text{ \AA}^2$, is smaller than expected for such a distance. The metrical parameters obtained from the curve fitting of the solution EXAFS obtained at +1.7 V are indistinguishable from those reported in Table 1 for the solution EXAFS at rest potential.

Discussion

The results obtained herein confirm the strikingly different

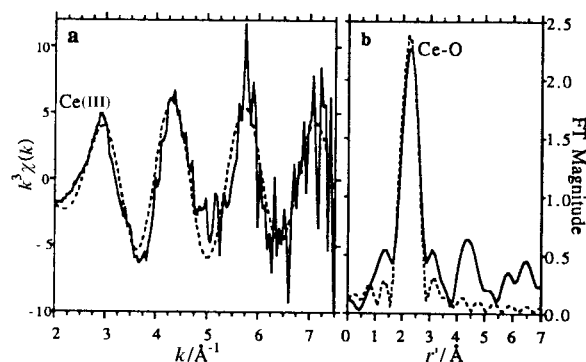


Fig. 5 *In situ* Ce L₂-edge (a) $k^3\chi(k)$ EXAFS and (b) FT data for the aqueous solution of $[\text{CeP}_5\text{W}_{30}\text{O}_{110}]^{12-}$ (5 mM) at the rest potential of +0.53 V. The solid lines are the primary experimental data and the dashed lines illustrate the fit.

redox behavior of the two Ce heteropolytungstate anions, $[\text{Ce}(\alpha\text{-}2\text{-P}_2\text{W}_{17}\text{O}_{61})_2]^{17-}$ and $[\text{CeP}_5\text{W}_{30}\text{O}_{110}]^{12-}$. The Wells–Dawson cluster stabilizes tetravalent Ce by about 1 V relative to the non-complexed aqua ion. The Preyssler anion stabilizes trivalent Ce, rendering it even more difficult to oxidize than in a non-complexing solution with similar pH. Two possible explanations for the different redox behavior may lie in the coordinating geometry of the Ce in the complexes and/or the charge stabilizing effects of the anion clusters. The *in situ* solution EXAFS results for $[\text{Ce}^{\text{III}}(\alpha\text{-}2\text{-P}_2\text{W}_{17}\text{O}_{61})_2]^{17-}$, $[\text{Ce}^{\text{IV}}(\alpha\text{-}2\text{-P}_2\text{W}_{17}\text{O}_{61})_2]^{16-}$, and $[\text{Ce}^{\text{III}}\text{P}_5\text{W}_{30}\text{O}_{110}]^{12-}$ provide insights into the apparent discrepancies in Ce redox behavior. It is argued that this behavior can be understood in terms of the coordination environments provided by these two heteropolyanions.

The EXAFS results demonstrate that the coordination of Ce in the Wells–Dawson and Preyssler anions is different. The average Ce(III)–O distance in $[\text{Ce}(\alpha\text{-}2\text{-P}_2\text{W}_{17}\text{O}_{61})_2]^{17-}$ is $2.52(4) \text{ \AA}$, which is essentially the same size as the sum of the Ce–O ionic radii for an 8-coordinate Ce and 2-coordinate O, 2.49 \AA .⁶³ This distance is typical of 8-coordinate cerium in oxidic compounds such as $\text{Ce}_2(\text{WO}_4)_3$, which has an average Ce(III)–O distance of 2.48 \AA ,⁶⁴ or Ce(III)–O in Ce_2MoO_6 , which has an average distance of 2.52 \AA .³⁹ In contrast, the average Ce(III)–O distance in $[\text{CeP}_5\text{W}_{30}\text{O}_{110}]^{12-}$ is $2.70(3) \text{ \AA}$, which is larger than the sum of the Ce–O ionic radii for 10-coordinate Ce and 3-coordinate oxygen (2.60 \AA), and the same as the similar sum for 12-coordinate Ce(III), 2.70 \AA . The structural refinements of Na⁺, Eu(III), and U(IV) in $[\text{P}_5\text{W}_{30}\text{O}_{110}]^{15-}$,^{54,65} suggest that Ce(III) is within the tunnel structure and bound to ten framework oxygen atoms. Our previous optical work on $[\text{EuP}_5\text{W}_{30}\text{O}_{110}]^{12-}$ demonstrated that the encrypted Eu is coordinated to either 2 or 3 H_2O molecules,³⁵ in addition to the 10 oxygen atoms expected from the anion itself. Precedent exists in the literature for the rather long Ce(III)–O bond length reported here, although only for 12-coordinate Ce. For example, the cubic perovskite CeVO_3 has Ce(III)–O bond distances of 2.758 \AA .⁶⁶

The crystallographically-determined mean Eu(III)–O₁₀ distances of $2.69(6)$ and $2.72(5) \text{ \AA}$ ⁵⁴ for two different salts of

[EuP₅W₃₀O₁₁₀]¹²⁻ are the same as the average distance determined here for the Ce analog. The independence of the Ln–O bond distance with the lanthanide ion size is attributed to the rigidity of the Preyssler anion framework. Based on the bond lengths observed here, the tunnel through the Preyssler structure is judged to be of more than adequate size to accommodate Ce(III) as depicted in Fig. 1b. Previous difficulties in preparing the large, light Ln (*i.e.*, La, Ce, Pr) derivatives of the Preyssler anion may have had more to do with the kinetics of the sluggish Na⁺ exchange reaction than with the inability of the anion to accommodate a large cation.^{12,67} This is evident from the ease with which tunnel-encapsulated Eu(III) is reduced to Eu(II)^{11,17} under essentially the same electrochemical conditions as employed herein for these studies of [CeP₅W₃₀O₁₁₀]¹²⁻.

Ce(III) is oxidized only in the Wells–Dawson framework. The Ce–O bond length contraction of 0.25 Å upon oxidation to Ce(IV) is substantial. The average Ce(IV)–O distance of 2.27(2) Å for the Wells–Dawson anion, [Ce(α-2-P₂W₁₇O₆₁)₂]¹⁶⁻, is short in comparison with the average Ce(IV)–O distance of 2.36(1) Å for the lacunary Linquist complex [Ce(W₅O₁₈)₂]^{18-,28}. Based upon the available X-ray diffraction results,^{20,22,28} both complexes contain 8-coordinate Ce(IV) in a square antiprism geometry. For coordination number 8, the ionic radii for Ce(III) and Ce(IV) are 1.143 and 0.97 Å, respectively.⁶³ The 0.173 Å difference between these ionic radii is smaller than the observed distance change of 0.25 Å between the Ce(III)–O and Ce(IV)–O bond lengths. This suggests that the contraction upon oxidation may be influenced by bonding effects between Ce and the O atoms from each of the two [α-2-P₂W₁₇O₆₁]¹⁰⁻ anions.¹⁸³ W NMR studies of [Ce(PW₁₁O₃₉)₂]¹¹⁻ suggest electron delocalization from Ce(III) onto adjacent W atoms through bridging O atoms, suggesting that the Ce–O–W bonding has covalent character.⁶⁸ The short Ce–O bonding in [Ce(α-2-P₂W₁₇O₆₁)₂]¹⁶⁻ might impart stability to this oxidized, Ce(IV) complex. The sandwich-like manner in which one Ce is coordinated between two Wells–Dawson anions (Fig. 1a) permits a conformational flexibility to the Ce environment, such that the anions are free to rotate and to move closer to or away from cerium as it changes valence.

The rigid framework of the Preyssler anion does not supply the encapsulated Ce ion with sufficient coordinating ligands to stabilize the tetravalent state. Ce(IV) has almost same ionic radius as Lu(III), and [LuP₅W₃₀O₁₁₀]¹²⁻ has been reported.⁸ Therefore, the ability of the complexed Ln-Preyssler anion to form is not entirely governed by the size of the central ion, but must be governed by the charge-to-radius ratio. A highly-charged small ion does not get the required stabilization from the surrounding O atoms, despite the overall large negative charge on the anion. That there can be effective charge transfer to the trivalent Ln ion is demonstrated by the previously published work on [EuP₅W₃₀O₁₁₀]¹²⁻.^{11,35} This work has shown that Eu(III), which is slightly smaller than Ce(III), can be reduced in the same environment. In fact, the reduction of encapsulated Eu(III) occurs at a more positive potential than the standard reduction potential for Eu(III), indicating that Eu(II) within the anionic Preyssler cluster of 15- charge is stabilized relative to the non-complexed aqua Eu(II) ion. This result is consistent with our argument that the size of the cation plays a dominant role over electrostatic considerations for the overall stability of the complex.

Taken together, these results point out the importance to the complex stability of fulfilling the coordination requirements of the Ln ion. We argue that the stabilizing effect of the Wells–Dawson anion on Ce(IV) is largely the result of its flexible structure. Although the cluster's large negative charge is important to the observed negative shift in the Ce(IV)/Ce(III) redox couple, the flexibility of the Wells–Dawson framework, which allows it to accommodate the smaller cation, plays a crucial role. Ce(III) is more difficult to oxidize in the Preyssler anion than it is in a

non-complexing solution because Ce(IV) is destabilized by its unfulfilled coordination requirements.

Conclusions

The redox behaviors of Ce in the Wells–Dawson and Preyssler anions are very different. Ce(IV) is stabilized in the former complex, with a formal potential of +0.37 V relative to the standard reduction potential of +1.52 V for the Ce(IV)/Ce(III) couple. In contrast, Ce(III) is not oxidized to Ce(IV) in the latter complex at applied potentials higher than those required to oxidize Ce(III) in a non-complexing electrolyte, which implies a stabilization of Ce(III) when it is complexed to the Preyssler anion. The ease of reduction of Eu(III), which is a slightly smaller cation than Ce(III), argues against a kinetic explanation that would involve difficulty in electron transfer between the [P₅W₃₀O₁₁₀]¹⁵⁻ framework and the encapsulated Ce ion.

The differences in stability of Ce(III) in the two highly-charged anions is understood in terms of the coordination environments provided by the Wells–Dawson and the Preyssler anions. The Wells–Dawson structure incorporates Ce(III) with a Ce–O bond distance that is typical of literature values. The framework structure is flexible and changes to accommodate the reduced size of the Ce(IV) ion, with a corresponding Ce–O distance that is again typical of literature values. In contrast, Ce(III) in the Preyssler anion has a Ce(III)–O bond distance of 2.7 Å, which is very long for a Ce–O interaction. The Ce–O distance found here is identical to that of the Eu(III)–O distance, although Eu is smaller than Ce. The similar distances found for these two f ions points to the rigidity of the Preyssler P–W–O framework. The failure to oxidize Ce(III) is then attributed to the larger charge-to-radius ratio for Ce(IV) over Ce(III), Lu(III) and Eu(II). Ce(IV) would not have coordination saturation in the Preyssler anion and, with its large charge, this destabilizes the tetravalent cation sufficiently that it will not form under the conditions of our electrochemical experiment. These results demonstrate the importance of an appropriately sized coordination environment, over those of electrostatic interactions, to the stability of heteropolyoxoanion complexes.

Acknowledgements

We thank Guy Jennings and S. Skanthakumar (ANL), Michaela Dankova and Judit Bartis (Hunter) for assistance. This work is supported by the U.S. DOE Basic Energy Sciences-Chemical Sciences under contract W-31-109-ENG-38 (MRA, LS, CWW) and by the Faculty Research Award Program of the City University of New York NSF-CHE9502213, NIH-Research Centers in Minority Institutions at Hunter College, Grant RR03037-08S2 (NU, LCF).

References

- 1 S. G. Bratsch, *J. Phys. Chem. Ref. Data*, 1989, **18**, 1.
- 2 A. W. Maverick and Q. Yao, *Inorg. Chem.*, 1993, **32**, 5626.
- 3 D. E. Hobart, K. Samhoun, J. P. Young, V. E. Norvell, G. Mamantov and J. R. Peterson, *Inorg. Nucl. Chem. Lett.*, 1980, **16**, 321.
- 4 D. W. Wester, G. J. Palenik and R. C. Palenik, *Inorg. Chem.*, 1985, **24**, 4435.
- 5 R. D. Peacock and T. J. R. Weakley, *J. Chem. Soc. A*, 1971, 1836.
- 6 L. McKean and M. T. Pope, *Inorg. Chem.*, 1974, **13**, 747.
- 7 J. P. Ciabrini and R. Contant, *J. Chem. Res. (S)*, 1993, 391.
- 8 I. Creaser, M. C. Heckel, R. J. Neitz and M. T. Pope, *Inorg. Chem.*, 1993, **32**, 1573.
- 9 N. Haraguchi, Y. Okaue, T. Isobe and Y. Matsuda, *Inorg. Chem.*, 1994, **33**, 1015.
- 10 T. Isobe and Y. Okaue, in *New Development of Studies on Rare Earth Complexes*, ed. G. Adachi, T. Yamase, J. Inanaga, M. Komiyama and K. Machida, The Rare Earth Society of Japan, Osaka, Japan, 1997, pp. 67–74.
- 11 M. R. Antonio and L. Soderholm, *J. Cluster Sci.*, 1996, **7**, 585.

- 12 M. R. Antonio, C. W. Williams and L. Soderholm, *J. Alloys Compd.*, 1998, **271**–**273**, 846.
- 13 M. T. Pope, *Heteropoly and Isopoly Oxometalates*, Springer-Verlag, Berlin, 1983.
- 14 M. T. Pope, in *Comprehensive Coordination Chemistry*, ed. G. Wilkinson, R. D. Gillard and J. A. McCleverty, Pergamon Press, New York, 1987, vol. 3, pp. 1023–1058.
- 15 M. T. Pope and A. Müller, *Angew. Chem., Int. Ed. Engl.*, 1991, **30**, 34.
- 16 M. T. Pope and A. Müller, *Polyoxometalates: From Platonic Solids to Anti-Retroviral Activity*, Kluwer, Dordrecht, 1994.
- 17 M. R. Antonio and L. Soderholm, *J. Alloys Compd.*, 1997, **250**, 541.
- 18 M. R. Antonio, L. Soderholm, L. C. Francesconi, M. Dankova and J. Bartis, *J. Alloys Compd.*, 1998, **275**–**277**, 827.
- 19 D. D. Dexter and J. V. Silverton, *J. Am. Chem. Soc.*, 1968, **90**, 3589.
- 20 J. Iball, J. N. Low and T. J. R. Weakley, *J. Chem. Soc., Dalton Trans.*, 1974, 2021.
- 21 V. I. Spitsyn, M. M. Orlova, N. N. Krot and A. S. Saprykin, *Russ. J. Inorg. Chem. (Transl. of Zh. Neorg. Khim.)*, 1978, **23**, 677.
- 22 V. N. Molchanov, L. P. Kazanskii, E. A. Torchenkova and V. I. Simonov, *Sov. Phys. Crystallogr. (Engl. Transl.)*, 1979, **24**, 96.
- 23 K. Nomiya, H. Murasaki and M. Miwa, *Polyhedron*, 1985, **4**, 1793.
- 24 W. H. Knoth, P. J. Domaille and R. L. Harlow, *Inorg. Chem.*, 1986, **25**, 1577.
- 25 M. R. Antonio and L. Soderholm, *Inorg. Chem.*, 1994, **33**, 5988.
- 26 L. G. Maksimova, T. A. Denisova, L. V. Kristallov, V. G. Kharchuk, N. A. Zhuravlev, V. L. Volkov and L. A. Petrov, *Russ. J. Inorg. Chem. (Transl. of Zh. Neorg. Khim.)*, 1995, **40**, 941.
- 27 M. T. Pope, X. Wei, K. Wassermann and M. H. Dickman, *C. R. Acad. Sci., Ser. IIc: Chim.*, 1998, **1**, 297.
- 28 C. Rosu and T. J. R. Weakley, *Acta Crystallogr., Sect. C*, 1998, **54**, CIF-access paper IUC9800047.
- 29 J. Bartis, M. Dankova, M. Blumenstein and L. C. Francesconi, *J. Alloys Compd.*, 1997, **249**, 56.
- 30 J. Bartis, S. Sukal, M. Dankova, E. Kraft, R. Kronzon, M. Blumenstein and L. C. Francesconi, *J. Chem. Soc., Dalton Trans.*, 1997, 1937.
- 31 M. T. Pope, in *Mixed-Valence Compounds. Theory, and Applications in Chemistry, Physics, Geology, and Biology*, ed. D. B. Brown, D. Reidel, Dordrecht, 1980, pp. 365–386.
- 32 L. Y. Qu, S. G. Wang, J. Peng, Y. G. Chen and G. Wang, *Polyhedron*, 1992, **11**, 2645.
- 33 L. Y. Qu, S. G. Wang, J. Peng, Y. G. Chen and M. Yu, *Chin. Sci. Bull.*, 1993, **38**, 1087.
- 34 X. Xi, G. Wang, B. Liu and S. Dong, *Electrochim. Acta*, 1995, **40**, 1025.
- 35 L. Soderholm, G. K. Liu, J. Muntean, J. Malinsky and M. R. Antonio, *J. Phys. Chem.*, 1995, **99**, 9611.
- 36 N. M. Edelstein, P. G. Allen, J. J. Bucher, D. K. Shuh, C. D. Soffield, N. Kaltsoyannis, G. H. Maunder, M. R. Russo and A. Sella, *J. Am. Chem. Soc.*, 1996, **118**, 13115.
- 37 J. S. Xue, M. R. Antonio, W. T. White, L. Soderholm and S. M. Kauzlarich, *J. Alloys Compd.*, 1994, **207**–**208**, 161.
- 38 R. Villanneau, A. Proust, F. Robert and P. Gouzerh, *J. Chem. Soc., Dalton Trans.*, 1999, 421.
- 39 M. R. Antonio, U. Staub, J. S. Xue and L. Soderholm, *Chem. Mater.*, 1996, **8**, 2673.
- 40 G. Bidoglio, P. N. Gibson, E. Haltier, N. Omenetto and M. Lipponen, *Radiochim. Acta*, 1992, **58**–**59**, 191.
- 41 C. Prieto, P. Lagarde, H. Dexpert, V. Briois, F. Villain and M. Verdager, *J. Phys. Chem. Solids*, 1992, **53**, 233.
- 42 T. K. Sham, *Phys. Rev. B: Condens. Matter*, 1989, **40**, 6045.
- 43 T. K. Sham, *J. Chem. Phys.*, 1983, **79**, 1116.
- 44 J. G. Darab, H. Li and J. D. Vienna, *J. Non-Cryst. Solids*, 1998, **226**, 162.
- 45 S.-L. Lin, C.-S. Hwang and J.-F. Lee, *J. Mater. Res.*, 1996, **11**, 2641.
- 46 S. Skanthakumar and L. Soderholm, *Phys. Rev. B: Condens. Matter*, 1996, **53**, 920.
- 47 R. F. Reidy and K. E. Swider, *J. Am. Ceram. Soc.*, 1995, **78**, 1121.
- 48 J. E. Sunstrom, S. M. Kauzlarich and M. R. Antonio, *Chem. Mater.*, 1993, **5**, 182.
- 49 S. H. Overbury, D. R. Huntley, D. R. Mullins and G. N. Glavee, *Catal. Lett.*, 1998, **51**, 133.
- 50 D. D. Beck, T. W. Capehart and R. W. Hoffman, *Chem. Phys. Lett.*, 1989, **159**, 207.
- 51 M. R. Antonio, J. F. Brazdil, L. C. Glaeser, M. Mehicic and R. G. Teller, *J. Phys. Chem.*, 1988, **92**, 2338.
- 52 A. J. Davenport, H. S. Isaacs and M. W. Kendig, *Proc. – Electrochem. Soc.*, 1991, **91**(7), 433.
- 53 A. J. Davenport, H. S. Isaacs and M. W. Kendig, *Corros. Sci.*, 1991, **32**, 653.
- 54 M. H. Dickman, G. J. Gama, K. C. Kim and M. T. Pope, *J. Cluster Sci.*, 1996, **7**, 567.
- 55 A. B. Yusov and V. P. Shilov, *Radiochemistry (New York)*, 1999, **41**, 1.
- 56 M. R. Antonio, L. Soderholm and I. Song, *J. Appl. Electrochem.*, 1997, **27**, 784.
- 57 F. W. Lytle, R. B. Gregor, D. R. Sandstrom, E. C. Marques, J. Wong, C. L. Spiro, G. P. Huffman and F. E. Huggins, *Nucl. Instrum. Methods Phys. Res., Sect. A*, 1984, **226**, 542.
- 58 F. W. Lytle, in *Applications of Synchrotron Radiation*, ed. H. Winick, D. Xian, M. H. Ye and T. Huang, Gordon and Breach, New York, 1989, vol. 4, pp. 135–223.
- 59 G. N. George and I. J. Pickering, “EXAFSPAK: A Suite of Computer Programs for Analysis of X-ray Absorption Spectra,” <http://www-ssrl.slac.stanford.edu/exafspak.html>.
- 60 J. M. de Leon, J. J. Rehr, S. I. Zabinsky and R. C. Albers, *Phys. Rev. B: Condens. Matter*, 1991, **44**, 4146.
- 61 J. J. Rehr, J. M. de Leon, S. I. Zabinsky and R. C. Albers, *J. Am. Chem. Soc.*, 1991, **113**, 5135.
- 62 A. W. Bott, *Curr. Sep.*, 1995, **14**, 64.
- 63 R. D. Shannon, *Acta Crystallogr., Sect. A*, 1976, **32**, 751.
- 64 T. Gressling and H. Müller-Buschbaum, *Z. Naturforsch., Teil B*, 1995, **50**, 1513.
- 65 M. H. Alizadeh, S. P. Harmalker, Y. Jeannin, J. M. Frere and M. T. Pope, *J. Am. Chem. Soc.*, 1985, **107**, 2662.
- 66 A. Wold and R. Ward, *J. Am. Chem. Soc.*, 1954, **76**, 1029.
- 67 M. R. Antonio, J. Malinsky and L. Soderholm, *Mater. Res. Soc. Symp. Proc.*, 1995, **368**, 223.
- 68 L. P. Kazansky and M. A. Fedotov, *J. Chem. Soc., Chem. Commun.*, 1983, 417.